



Marian Klasztorny*, Piotr Szurgott, Tadeusz Niezgodą, Danuta Miedzińska, Andrzej Kiczko

Military University of Technology, Faculty of Mechanical Engineering, Department of Mechanics and Applied Computer Science

ul. gen. S. Kaliskiego 2, 00-908 Warsaw, Poland

**Corresponding author. E-mail: m.klasztorny@gmail.com*

Received (Otrzymano) 24.02.2017

PRELIMINARY COMPARATIVE STATIC IDENTIFICATION RESEARCH ON SELECTED COMMERCIAL AUXETIC FABRICS

Preliminary comparative static identification experimental tests on four selected commercial auxetic woven fabrics were conducted in terms of the tensile test in the auxetic fibre direction. A new method of such tests was developed, based on capstan grips as well as on video-extensometer and extensometer techniques. The identification tests were carried out at temperatures of 20 and 180°C due to the intended use of auxetic fabric as a protective curtain against a shock wave induced by a gas explosion. The ultimate tension force per unit width of fabric, effective Poisson's ratios in the fabric plane and in the transverse plane, as well as the absorbed energy were determined approximately. The auxetic fabric with the relatively best properties was selected.

Keywords: auxetic fabric, energy absorption, material properties, preliminary research, tensile test, static identification

WSTĘPNE PORÓWNAWCZE STATYCZNE BADANIA IDENTYFIKACYJNE WYBRANYCH AUKSETYCZNYCH TKANIN UŻYTKOWYCH

Przeprowadzono wstępne porównawcze statyczne doświadczalne testy identyfikacyjne czterech wybranych auksetycznych tkanin użytkowych w zakresie próby rozciągania w kierunku włókna auksetycznego. Została opracowana nowa metoda takich badań, wykorzystująca uchwyty kabestanowe, jak również wideotensometr i techniki tensometryczne. Testy identyfikacyjne prowadzono w temperaturach 20 i 180°C, ze względu na planowane zastosowanie materiału auksetycznego w postaci kurtyny ochronnej przeciw fali uderzeniowej wywołanej wybuchem gazu. Na podstawie testów określono graniczną nośność tkaniny, efektywne wartości współczynnika Poissona w płaszczyźnie tkaniny i w płaszczyźnie poprzecznej oraz energię absorbowaną. Wybrano tkaninę auksetyczną charakteryzującą się względnie najlepszymi właściwościami.

Słowa kluczowe: tkaniny auksetyczne, pochłanianie energii, właściwości materiałowe, badania wstępne, próba rozciągania, identyfikacja statyczna

INTRODUCTION

A typical plain weave auxetic fabric is composed of auxetic yarns as the weft and conventional fibres (interlacement) as the warp. An auxetic fibre is wound in a double helix, and contains a thin, high-strength spiral wrap with high-stiffness and a thick elastomeric core. Under tension in the yarn direction, the spiral wrap tends to straighten, which causes bending of the core resulting in a negative effective Poisson's ratio. Hence, the elastomeric core absorbs energy by bending itself. Changes in the wrap angle during tension of the auxetic fibres result in effective Young's modules and effective Poisson's ratios dependent on the strains. The main advantages of auxetic materials include increased shear stiffness, a double synclastic curvature in bending, an increase in the fracture strength, increased resistance to dents, and increased damping [1, 2]. The mechanical properties of auxetic yarns and fabrics have

been investigated experimentally, analytically or numerically in a number of papers. The results of the tensile test of a single auxetic fibre are presented by Wright et al. [1]. The yarn was subjected to six load-unload cycles up to blocking the transverse displacements due to complete straightening of the spiral wrap. The best auxetic fibres were identified in a group of the fibres under consideration. Static tests on the energy absorption of a fabric strip were conducted using a device for measuring the vertical displacement of fabric caused by stretching in the weft direction up to failure. The absorbed energy was calculated based on the force-displacement graph.

A new composite with the use of auxetic fibres in order to obtain an auxetic composite was developed by Miller et al. [2]. A wrap made of UHMWPE (Ultra High Molecular Weight Polyethylene) and an elas-

tomeric polyurethane core were used. A single auxetic fibre has a negative effective Poisson's ratio up to -2.1 . A plain weave fabric was manufactured using a meta-aramid fibre as the warp and a silicone rubber gel as the matrix. The fabric samples were prepared and subjected to stretching in the auxetic fibre direction.

Wright et al. [3] determine numerically the mechanical properties of an auxetic yarn, composed of a core and a wrap, based on the tensile test. The finite element method (FEM) and commercial software ABAQUS V6.8-3 were applied. In the contact model, tie constraints were assumed (no slip or friction). The authors studied the influence of various design parameters on the behaviour of the auxetic yarn, i.e., the core-to-wrap diameter ratio, the wrap angle, as well as Young's modules and Poisson's ratios of both components.

Sloan et al. [4] present experimental research on the mechanical properties of helical auxetic yarn (HAY). The effect of the wrap angle on these properties was determined. Miller et al. [5] describe the manufacture of an auxetic composite reinforced unidirectionally with yarns composed of carbon fibre (the wrap) and nylon (the core). Experimental tests were performed according to ASTM WK12919 (characterisation of a single fibre) and ASTM D3039/D 3039M (tensile properties of polymer-matrix composite materials) standards. On the basis of the strains recorded during the tests, effective Poisson's ratios within the range of (-6) to 1 were determined. The auxetic effect is fully revealed in the case of an auxetic fabric loaded transversely by a shock wave from a gas explosion or explosive charge [1]. For a rectangular auxetic fabric fixed along all the edges, the shock wave induces a transverse displacement surface with a double synclastic curvature.

So far, several auxetic structures based on concave hexagons or quadrangles (protected by patents) with a bar or plate structure (triangles or rectangles) have been developed [6, 7]. Moreover, knitted structures based on the fundamental auxetic hexagonal pattern have been developed [6, 8, 9]. A single auxetic fibre, in the form of a double helix, is mostly tested [1, 3, 4, 10, 11]. The results of the studies refer to a cylinder comprising an auxetic fibre in the tensile test. For auxetic fabric the results are usually different because of the effect of the tense string of the stretched wrap without the possibility of in-plane transverse displacement due to blocking of the fabric sample in the jaws of a testing machine [7]. It induces effective normal stresses in the in-plane transverse direction. Polymer-matrix composites reinforced with auxetic fibres or auxetic fabrics are in the early stages of development [5].

The literature review has also revealed that FEM simulations for auxetic materials have been performed on the micro scale (on a single auxetic fibre), on the meso scale (on a representative cell of the material), and on the macro scale (on a fabric sample) [3, 10, 11]. The influence of the geometry and material parameters

on the mechanical properties of auxetic fabrics has been investigated. A characteristic feature is observed in the form of a strong non-linear dependence of the effective Poisson's ratios on the geometry of an auxetic material, including transition from negative values to positive ones and vice versa. Significantly high negative values of the effective Poisson's ratio up to -8 can be achieved by respective modifications of the fabric geometry. The modelling was conducted using the computer code ANSYS.

The study presents preliminary comparative experimental static identification research on four selected commercial auxetic woven fabrics in terms of the tensile test in the auxetic fibre direction. A new method of such tests based on capstan grips as well as on video-extensometer and extensometer techniques was developed. The identification tests were carried out at the temperatures of 20 and 180°C due to the intended application of auxetic woven fabric as a curtain against the shock wave of a gas explosion. Approximate values of the ultimate tension force per unit width of a fabric, effective Poisson's ratios in the fabric plane and in the transverse plane, and the absorbed energy in tensile tests were determined. The auxetic woven fabric with the relatively best properties was selected. Exact identification based on statistical analysis is planned in further research.

MATERIAL SPECIFICATIONS AND EXPERIMENTAL RESEARCH METHOD

Four types of auxetic woven fabrics, commercially available nowadays in England for explosion-proof curtains applications, are considered in the current study. The fabrics were proposed by the manufacturers. Their components are listed in Table 1.

Based on the results of the explosion-proof curtain studies described in [1], the authors of Ref. [1] found that the following materials revealed the best energy-absorption properties:

1. warp fibres: Conex® (meta-aramid)
2. spiral wrap: twisted Dyneema® fibres with improved tension control during wrapping
3. elastomeric core: red polyurethane elastomeric fibres.

The above mentioned components are different from those considered in this study (Table 1).

The tensile tests in the auxetic fibre direction were performed on two samples for each fabric, using an INSTRON 8862 testing machine. LaborTech TH224080 capstan grips, instead of conventional grips, were used. This approach, applied to seat-belt testing, eliminates the tension-compression state at the ends of strip samples of auxetic fabrics. A strip sample is wound on two rolls of a 40 mm diameter and 80 mm length as shown in Figure 1, employing two wraps.

The displacement-controlled tests were conducted at a 50 mm/min crosshead velocity. The signals were recorded at a frequency of 25 Hz until load capacity

loss of the sample. The tests were carried out at the temperatures of 20 and 180°C. The elevated temperature was specified by the Fire Service College - Cra-cow, a partner in the Project noted in the Acknowl-edgements. For the tests at the elevated temperature, the environmental temperature was raised at the rate of 1°C/min and then the sample was left for 5 minutes at 180°C in a thermal chamber.

TABLE 1. Components and some properties of auxetic fabrics (AF) selected for experimental tests

TABELA 1. Skład i niektóre właściwości tkanin auksetycznych wybranych do badań doświadczalnych

Parameter		Auxetic fabric AF1	Auxetic fabric AF2	Auxetic fabric F3	Auxetic fabric AF4
Warp fibres		DuPont Kevlar 29 (3000 den)	glass fibre with stainless steel wire inclusions	para-aramid Twaron Type 2200 (1100 dtex)	ballistic Nylon 6-6 HT (940 dtex)
Auxetic yarns (weft direction)	Spiral wrap	DuPont Kevlar 129 (1670 dtex)	DuPont Kevlar (777 dtex)	Twaron Type 2200 (1100 dtex)	Honeywell Spectra 1000 (375 den)
	Elasto-meric core	0.6 mm diameter, elastomeric polyester monofilament			
Weight		700 gsm	820 gsm	650 gsm	650 gsm
Remarks		—	higher fire resistance	—	resistant to UV radiation

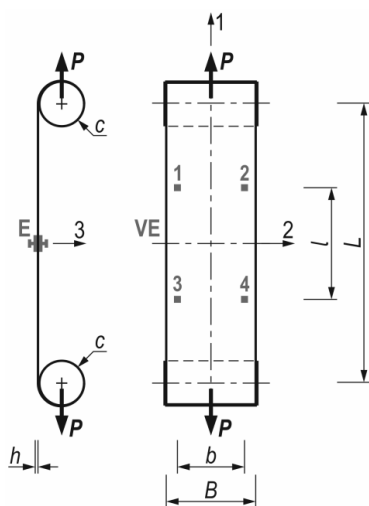


Fig. 1. Fastening of fabric sample using capstan grips and location of test markers (E - extensometer, VE - video-extensometer, c - roller radius)

Rys. 1. Sposób mocowania próbki tkaniny w uchwytach kabestanowych oraz rozmieszczenie znaczników (E - ekstensometr, VE - video-ekstensometr, c - promień rolki)

The following devices were used to perform the tensile tests:

1. a video-extensometer (a Phantom v12 high-speed camera) to measure the longitudinal and transverse elongations, based on four 2×2 mm square markers

on a fabric strip and TEMA software used for the identification,

2. an extensometer with platelets at the ends for strain measurement in the thickness direction of the fabric,
3. a thermal chamber assembled with an INSTRON 8862 testing machine.

The following principal directions of an auxetic fabric are assumed: 1 - auxetic yarn direction, 2 - warp direction, 3 - thickness direction. The following symbols are adopted (see Fig. 1):

L - sample length between the contact points with the capstan grips,

l - axial distance between the markers in the vertical direction

Δl - elongation of section l ,

Δl_{max} - ultimate elongation of section l ,

B - sample width,

b - axial distance between the markers in the horizontal direction,

Δb - elongation of section b ,

h - fabric thickness before the tensile test (measured between the platelets at the ends of the extensometer),

Δh - thickening of section h ,

P - tension force,

s - crosshead displacement. The dimensions of the fabric samples are: $L_0 = 700$ mm, $B = 80$ mm, $L = 200$ mm, $l = 100$ mm, $b = 60$ mm,

The following output quantities were determined:

S_1 - tensile force in direction 1 per unit length of fabric in direction 2, identified as the force intensity [N/m],

S_{1max} - maximum tensile force in direction 1 per unit length of fabric in direction 2 [N/m],

ϵ_1 - average strain in direction 1 at the measuring length of l (measured from test markers 1, 3 and 2, 4),

ϵ_2 - average strain in direction 2 at the measuring length of b (measured from test markers 1, 2 and 3, 4),

ϵ_3 - average strain in direction 3 at the measuring length of h ,

ν_{12} - effective in-plane Poisson's ratio (contraction in direction 2 under tension in direction 1),

ν_{13} - effective transverse Poisson's ratio (contraction in the direction 3 under tension in direction 1),

E_{a1} - energy absorbed during tension of section l in direction 1, per unit length of fabric in direction 2 [J/m].

The following signals were recorded during each test: s [mm], P [N], Δl [mm], Δb [mm], Δh [mm], wherein Δl and Δb were recorded in two possible variants resulting from the marker locations.

The output quantities were calculated from the following formulae:

$$S_1 = \frac{P}{B} \tag{1}$$

$$\epsilon_1 = \frac{\Delta l}{l}, \epsilon_2 = \frac{\Delta b}{b}, \epsilon_3 = \frac{\Delta h}{h} \tag{2}$$

$$\nu_{12} = \frac{\varepsilon_2}{\varepsilon_1}, \nu_{13} = \frac{\varepsilon_3}{\varepsilon_1} \quad (3)$$

$$E_{d1} = \int_0^{\Delta l_{\max}} S_1(\Delta l) d\Delta l \quad (4)$$

Based on the recording, the following graphs were determined: $S_1(\Delta l)$, $\nu_{12}(\varepsilon_1)$, $\nu_{13}(\varepsilon_1)$.

RESULTS OF EXPERIMENTAL TESTS AND DISCUSSION

The stand for the identification tests is depicted in Figures 2-4. The AF1 samples are presented as an example for the two temperature levels.



Fig. 2. AF1 fabric sample mounted in capstan grips; test at temperature T_1
Rys. 2. Próbkę tkaniny AF1 umieszczoną w uchwytach kabestanowych; próba w temperaturze T_1

Figure 5 shows graphs $S_1(\Delta l)$ at room (T_1) and elevated (T_2) temperatures, for the tested fabrics. Based on these graphs, the following quantities were determined: the maximum tensile force in the direction 1 per unit length of fabric in the direction 2 (force intensity, $S_{1\max}$), energy absorbed during tension of section l in the direction 1, per unit length of fabric in direction 2, up to load capacity point $S_{1\max}$. Figures 6-13 present the

graphs of effective Poisson's ratios $\nu_{12}(\varepsilon_1)$, $\nu_{13}(\varepsilon_1)$ corresponding to fabrics AF1, AF2, AF3, AF4, at temperatures T_1 and T_2 .

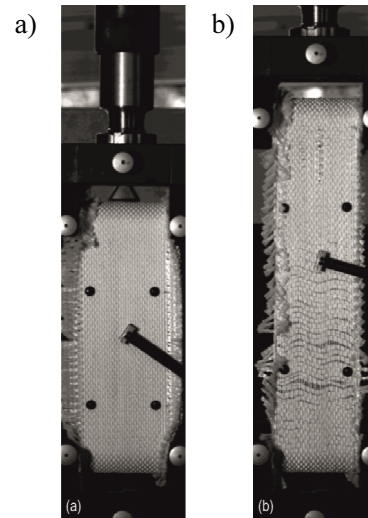


Fig. 3. AF1 fabric sample during tensile test at temperature T_1 : before (a) and after (b) test

Rys. 3. Próbkę tkaniny AF1 podczas próby rozciągania w temperaturze T_1 : przed (a) i po (b) próbie

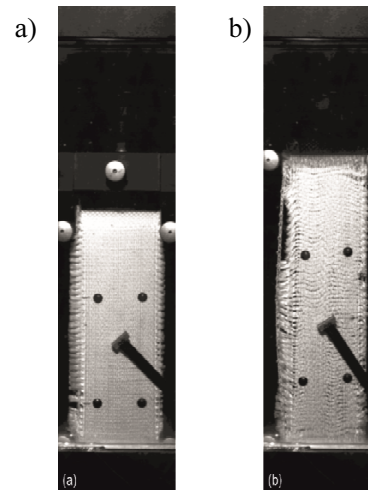


Fig. 4. AF1 fabric sample during tensile test at temperature T_2 : before (a) and after (b) test

Rys. 4. Próbkę tkaniny AF1 podczas próby rozciągania w temperaturze T_2 : przed (a) i po (b) próbie

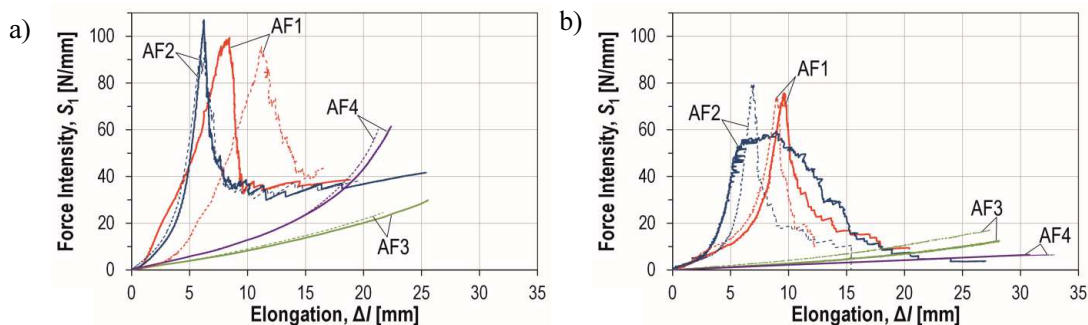


Fig. 5. Influence of fabric type on $S_1(\Delta l)$ graph. Tests at room temperature T_1 (a) and elevated temperature T_2 (b): sample 1 - solid line, sample 2 - dashed line

Rys. 5. Wpływ rodzaju tkaniny na zależność $S_1(\Delta l)$. Próba w temperaturze pokojowej T_1 (a) i podwyższonej T_2 (b): próbka 1 - linia ciągła, próbka 2 - linia przerywana

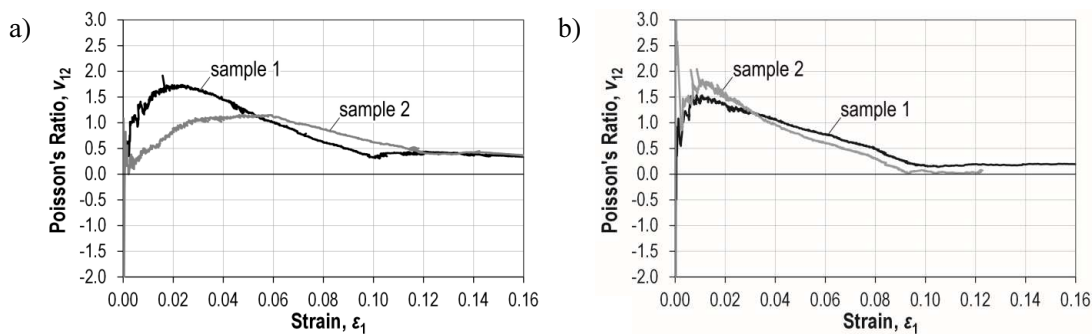


Fig. 6. Effective Poisson's ratio $\nu_{12}(\varepsilon_1)$ for AF1 auxetic fabric. Tests at room temperature T_1 (a) and elevated temperature T_2 (b)

Rys. 6. Efektywny współczynnik Poissona $\nu_{12}(\varepsilon_1)$ dla tkaniny auksetycznej AF1. Próba w temperaturze pokojowej T_1 (a) i podwyższonej T_2 (b)

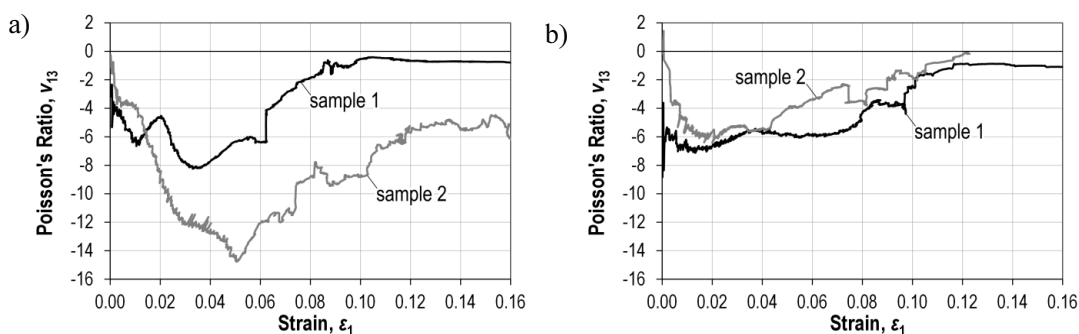


Fig. 7. Effective Poisson's ratio $\nu_{13}(\varepsilon_1)$ for AF1 auxetic fabric. Tests at room temperature T_1 (a) and elevated temperature T_2 (b)

Rys. 7. Efektywny współczynnik Poissona $\nu_{13}(\varepsilon_1)$ dla tkaniny auksetycznej AF1. Próba w temperaturze pokojowej T_1 (a) i podwyższonej T_2 (b)

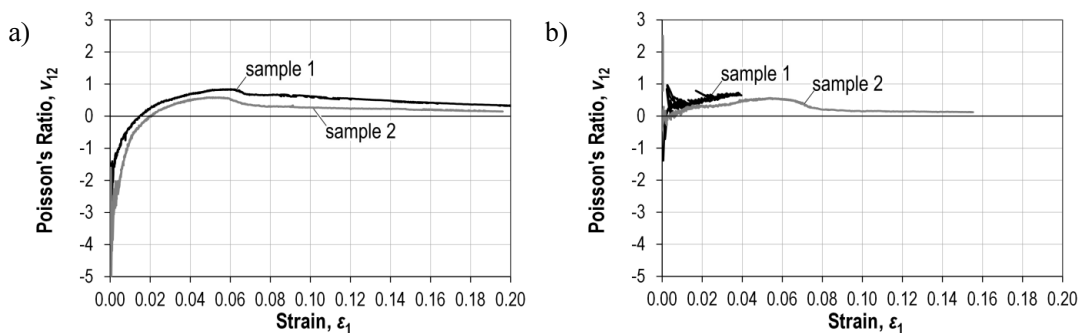


Fig. 8. Effective Poisson's ratio $\nu_{12}(\varepsilon_1)$ for AF2 auxetic fabric. Tests at room temperature T_1 (a) and elevated temperature T_2 (b)

Rys. 8. Efektywny współczynnik Poissona $\nu_{12}(\varepsilon_1)$ dla tkaniny auksetycznej AF2. Próba w temperaturze pokojowej T_1 (a) i podwyższonej T_2 (b)

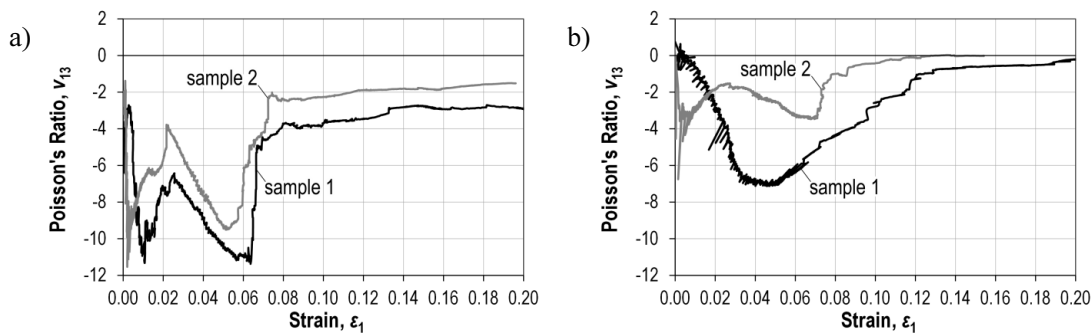


Fig. 9. Effective Poisson's ratio $\nu_{13}(\varepsilon_1)$ for AF2 auxetic fabric. Tests at room temperature T_1 (a) and elevated temperature T_2 (b)

Rys. 9. Efektywny współczynnik Poissona $\nu_{13}(\varepsilon_1)$ dla tkaniny auksetycznej AF2. Próba w temperaturze pokojowej T_1 (a) i podwyższonej T_2 (b)

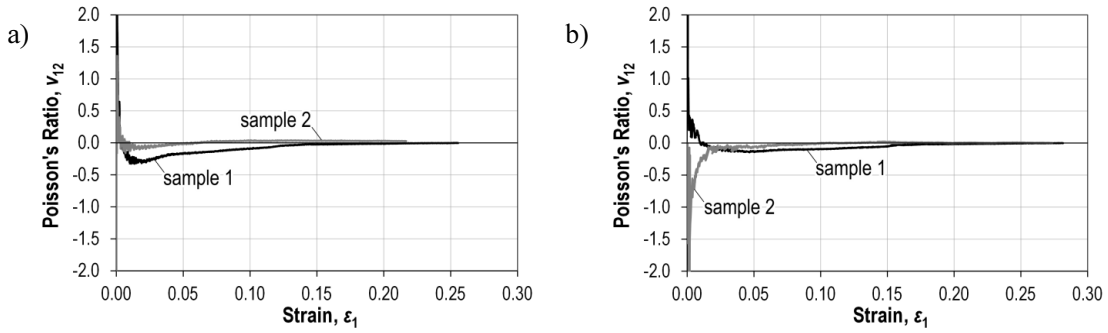


Fig. 10. Effective Poisson's ratio $\nu_{12}(\epsilon_1)$ for AF3 auxetic fabric. Tests at room temperature T_1 (a) and elevated temperature T_2 (b)
 Rys. 10. Efektywny współczynnik Poissona $\nu_{12}(\epsilon_1)$ dla tkaniny auksetycznej AF3. Próba w temperaturze pokojowej T_1 (a) i podwyższonej T_2 (b)

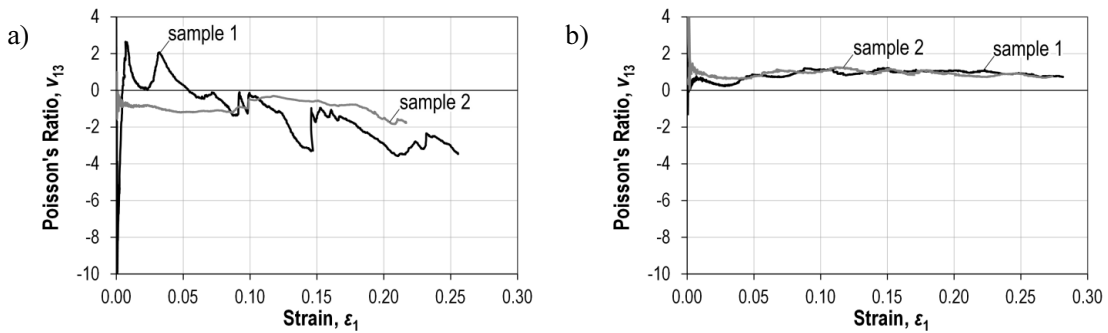


Fig. 11. Effective Poisson's ratio $\nu_{13}(\epsilon_1)$ for AF3 auxetic fabric. Tests at room temperature T_1 (a) and elevated temperature T_2 (b)
 Rys. 11. Efektywny współczynnik Poissona $\nu_{13}(\epsilon_1)$ dla tkaniny auksetycznej AF3. Próba w temperaturze pokojowej T_1 (a) i podwyższonej T_2 (b)

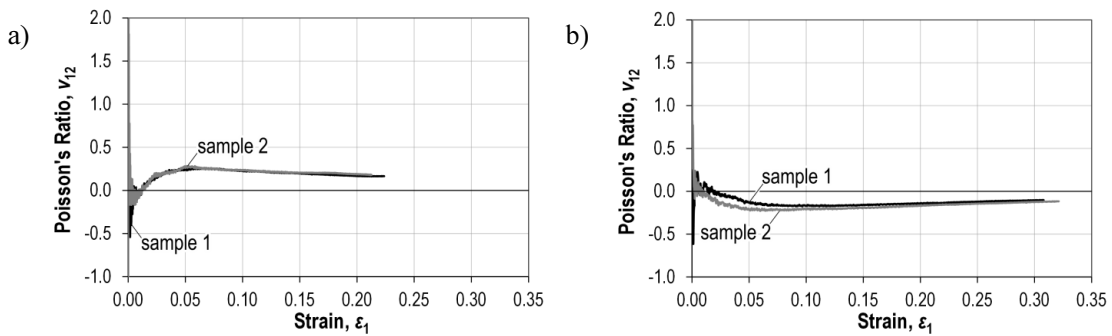


Fig. 12. Effective Poisson's ratio $\nu_{12}(\epsilon_1)$ for AF4 auxetic fabric. Tests at room temperature T_1 (a) and elevated temperature T_2 (b)
 Rys. 12. Efektywny współczynnik Poissona $\nu_{12}(\epsilon_1)$ dla tkaniny auksetycznej AF4. Próba w temperaturze pokojowej T_1 (a) i podwyższonej T_2 (b)

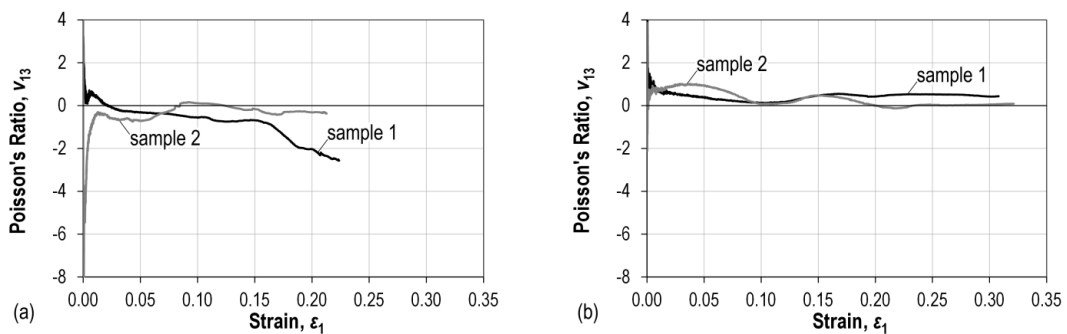


Fig. 13. Effective Poisson's ratio $\nu_{13}(\epsilon_1)$ for AF3 auxetic fabric. Tests at room temperature T_1 (a) and elevated temperature T_2 (b)
 Rys. 13. Efektywny współczynnik Poissona $\nu_{13}(\epsilon_1)$ dla tkaniny auksetycznej AF3. Próba w temperaturze pokojowej T_1 (a) i podwyższonej T_2 (b)

The numerical results of the tensile tests presented in Table 2 include: $S_{1\max}$, Δl_u , a range of $\nu_{12}(\varepsilon_1)$ values, a range of $\nu_{13}(\varepsilon_1)$ values, E_{a1} . The output quantities are calculated as the average values for two samples. They are approximate estimations as only two specimens were tested for each fabric.

The fundamental characteristic obtained as a result of the tensile strength tests is a graph of the tension force intensity versus elongation of the measuring section, $S_1(\Delta l)$. This characteristic is described below for the four tested fabrics. Percentage increases/decreases are calculated for the average values for two samples of each fabric at a given temperature.

The $S_1(\Delta l)$ characteristic for the AF1 fabric exhibited good qualitative compatibility and good compatibility in the load capacity. However, a large discrepancy of the ultimate elongation was detected (Fig. 5). This characteristic is nonlinearly elastic with a progressive gradient to the point of load capacity, followed by progressive destruction of a moderate gradient decline, passing into the plateau phase at the load intensity level of 40 N/mm. **Compared to the room temperature conditions, the elevated temperature conditions induce a load capacity reduction of about 13% and an absence of the plateau phase.** The AF1 samples are resistant to the elevated temperature.

TABLE 2. Results of tensile tests of AF1-AF4 auxetic fabrics
TABELA 2. Wyniki prób rozciągania tkanin auksetycznych AF1-AF4

Fabric	Temperature	$S_{1\max}$ [N/mm]	Δl_u [mm]	range $\nu_{12}(\varepsilon_1)$	range $\nu_{13}(\varepsilon_1)$	E_{a1} [J/m]
AF1	T_1	97.5	9.8	[+0.15; +1.53]	[-11.5; -0.58]	334
	T_2	74.8	9.4	[+0.07; +1.79]	[-6.77; -0.57]	170
AF2	T_1	100.0	6.1	[-3.20; +0.72]	[-11.4; -1.90]	156
	T_2	79.6	6.8	[-0.11; +0.57]	[-6.76; -0.03]	182
AF3	T_1	27.2	23.6	[-0.24; +0.83]	[-5.01; +1.30]	273
	T_2	14.8	27.7	[-5.83; +0.22]	[-0.03; +5.58]	164
AF4	T_1	60.8	21.8	[-0.35; +0.52]	[-4.02; +0.69]	410
	T_2	6.5	31.8	[-0.42; +0.24]	[-0.02; +1.25]	109

The $S_1(\Delta l)$ characteristic for the AF2 fabric was repeatable. This fabric exhibits less resistance to the elevated temperature as the results for the two samples differ substantially (Fig. 5). This characteristic is nonlinearly elastic with a progressive gradient to the point of load capacity, followed by progressive destruction of a considerable gradient decline, passing into the plateau phase at the load intensity level of 40 N/mm. **Compared to the room temperature conditions, the elevated temperature conditions induce**

a load capacity reduction of about 20% and an absence of the plateau phase.

The $S_1(\Delta l)$ characteristic for the AF3 fabric showed good qualitative compatibility, and moderate compatibility in the load capacity and the ultimate elongation (Fig. 5). This characteristic is nonlinearly elastic with a progressive gradient to the point of load capacity, followed by rupture. **Compared to the room temperature conditions, the elevated temperature conditions induce a load capacity reduction of about 46%.** The samples are resistant to the elevated temperature.

The $S_1(\Delta l)$ characteristic of the AF4 fabric revealed good qualitative and quantitative compatibility (Fig. 5). This characteristic is nonlinearly elastic with a progressive gradient to the point of load capacity, followed by rupture of the sample. **Compared to the room temperature conditions, the elevated temperature conditions induce a substantial load capacity reduction of about 89%.** The samples are resistant to the elevated temperature.

The in-plane effective Poisson's ratio, $\nu_{12}(\varepsilon_1)$, depended non-linearly on the strain of auxetic fibres. At room temperature, this ratio took negative values for fabrics AF2, AF3, AF4 in the initial phase of tension, and passed to positive values for the next phase. At the elevated temperature, these fabrics behaved similarly, but the ranges of Poisson's ratio differed from those obtained at room temperature. The greatest effect of the negative Poisson's ratio, $\nu_{12}(\varepsilon_1)$, was revealed for the AF3 fabric at the elevated temperature. Negative values of ratio $\nu_{12}(\varepsilon_1)$ did not occur in the AF1 fabric either at room or elevated temperatures.

Negative values of effective Poisson's ratio $\nu_{13}(\varepsilon_1)$ occurred in the all tested fabrics, at both room and elevated temperatures. Nonetheless, the temperature of 180°C significantly reduces or almost completely eliminates this effect. The extremum negative values of Poisson's ratio $\nu_{13}(\varepsilon_1)$, resulting in thickening of the fabric during tension in the auxetic fibre direction, was detected in the AF1 fabric.

The $S_1(\Delta l)$ characteristics corresponding to the four tested fabrics are compared in Figure 5, at the temperatures of 20°C and 180°C. The AF1 fabric was selected as the relatively best for gas explosion-proof applications due to the following advantages:

1. a high load capacity (force intensity) $S_{1\max} = 97.5$ N/mm at the ultimate elongation of ~ 10 mm
2. good progression of the hard non-linear elastic characteristic
3. extremum negative values of Poisson's ratio $\nu_{13}(\varepsilon_1)$
4. high load capacity (force intensity) in the plateau phase, ~ 40 N/mm
5. high energy absorption, 334 J/m
6. high resistance to temperatures up to 180°C
7. a low drop by 13% in the load capacity (force intensity) at the elevated temperature (180°C) compared to the room temperature.

CONCLUSIONS

Preliminary comparative experimental static identification tests conducted within the current study concern four selected auxetic woven fabrics. Tensile strength tests in the auxetic fibre direction were performed. The method of such tests, based on capstan grips and video-extensometer and extensometer techniques, has proven effective in determining the approximate values of the ultimate tension force per unit width of fabric, the effective Poisson's ratios in the fabric plane and in the transverse plane, and the energy absorbed by a fabric.

Compared to the results of the reviewed references, the study contains the following new elements:

1. a new methodology for tensile tests of auxetic woven fabrics
2. tensile tests for four commercial auxetic woven fabrics (the producers do not provide the data for the parameters identified by the authors)
3. performing tensile tests at the room temperature of 20°C and elevated temperature of 180°C
4. selection of the optimal auxetic woven fabric based on energy-absorption criterion.

It has been shown that the values of Poisson's ratio ν_{12} for an auxetic woven fabric differ significantly from the values of this ratio for relevant single auxetic yarn under tension. Exact analysis should be based on at least 5 samples in each test. The tense string effect induced blocking of the negative in-plane Poisson's ratio effect. On the other hand, the negative transverse Poisson's ratio effect was not blocked.

The identification was carried out at the temperatures of 20 and 180°C due to the intended application of the preferred auxetic woven fabric as a curtain against a shock wave induced by a gas explosion. The ultimate tensile force per unit width of the fabric strip, in-plane and transverse effective Poisson's ratios, and the absorbed energy were defined and determined approximately for each fabric.

Based on the comparative analysis, it was demonstrated that the AF1 fabric has the relatively best properties and is recommended for gas explosion-proof curtain applications. These applications are planned to be developed in further research.

Acknowledgements

The study was supported by the National Centre for Research and Development, Poland, as a part of research project No. DOB-BIO6/04/104/2014 (acronym THERMOTEX), financed in the period 2014-2017. This support is gratefully acknowledged.

REFERENCES

- [1] Wright J.R., Evans K.E., Burns M.K., Auxetic blast protection textiles - Crime feasibility study, Final Report - EP/D036690/1, University of Exeter, Great Britain 2007.
- [2] Miller W., Hook P.B., Smith C.W., Wang X., Evans K.E., The manufacture and characterisation of a novel, low modulus, negative Poisson's ratio composite, *Compos. Sci. Technol.* 2009, 69:5, 651-655.
- [3] Wright J.R., Sloan M.R., Evans K.E., Tensile properties of helical auxetic structures: A numerical study, *J. Appl. Phys.* 2010, 108, 044905.
- [4] Sloan M.R., Wright J.R., Evans K.E., The helical auxetic yarn - A novel structure for composites and textiles; geometry, manufacture and mechanical properties, *Mech. Mater.* 2011, 43, 9, 476-486.
- [5] Miller W., Ren Z., Smith C.W., Evans K.E., A negative Poisson's ratio carbon fibre composite using a negative Poisson's ratio yarn reinforcement, *Compos. Sci. Technol.* 72, 2012, 7, 761-766.
- [6] Rant D., Rijavec T., Pavko-Cuden A., Auxetic textiles, *Acta. Chim. Slov.* 2013, 60, 4, 715-723.
- [7] Hu H., Wang Z., Liu S., Development of auxetic fabrics using flat knitting technology, *Text. Res. J.* 2011, 81, 14, 1493-1502.
- [8] Ugbohue S.C., Kim Y.K., Warner S.B., Fan Q., Yang C.L., Kyzymchuk O., Feng Y., The formation and performance of auxetic textiles. Part I: theoretical and technical considerations, *J. Text. I* 2010, 101, 7, 660-667.
- [9] Ugbohue S.C., Kim Y.K., Warner S.B., Fan Q., Yang C.L., Kyzymchuk O., Feng Y., The formation and performance of auxetic textiles. Part II: geometry and structural properties, *J. Text. I* 2010, 102:5, 424-433.
- [10] Ge Z., Hu H., Liu Y., A finite element analysis of a 3D auxetic textile structure for composite reinforcement, *Smart Mater. Struct.* 2012, 22, 084005.
- [11] Shen Y., Modeling of Tensile Properties of Woven Fabrics and Auxetic Braided Structures by Multi-Scale Finite Element Method, M.Sc. Thesis, Auburn University, United States 2013.